Tryptophan Solvent Exposure in Folded and Unfolded States of an SH3 Domain by ^{19}F and ^{1}H NMR†

Ferenc Evanics,‡ Irina Bezsonova,‡,§ Joseph Marsh,§,|| Julianne L. Kitevski,‡ Julie D. Forman-Kay,§,|| and R. Scott Prosser*,‡

Department of Chemistry, University of Toronto, Toronto, Canada, Molecular Structure and Function Program, Hospital for Sick Children, Toronto, Canada, and Department of Biochemistry, University of Toronto, Toronto, Canada

Received July 10, 2006; Revised Manuscript Received September 11, 2006

ABSTRACT: The isolated N-terminal SH3 domain of the *Drosophila* signal transduction protein Drk (drkN SH3) is a useful model for the study of residual structure and fluctuating structure in disordered proteins since it exists in slow exchange between a folded (F_{exch}) and compact unfolded (U_{exch}) state in roughly equal proportions under nondenaturing conditions. The single tryptophan residue, Trp36, is believed to play a key role in forming a non-native hydrophobic cluster in the U_{exch} state, with a number of long-range nuclear Overhauser contacts (NOEs) observed primarily to the indole proton. Substitution of Trp36 for 5-fluoro-Trp36 resulted in a substantial shift in the equilibrium to favor the F_{exch} state. A variety of ^{19}F NMR measurements were performed to investigate the degree of solvent exposure and hydrophobicity associated with the 5-fluoro position in both the F_{exch} and U_{exch} states. Ambient T_1 measurements and H_2O/D_2O solvent isotope effects indicated extensive protein contacts to the 5-fluoro position in the F_{exch} state and greater solvent exposure in the U_{exch} state. This was corroborated by the measurements of paramagnetic effects (chemical shift perturbations and T_1 relaxation enhancement) from dissolved oxygen at a partial pressure of 20 atm. In contrast, paramagnetic effects from dissolved oxygen revealed less solvent exposure to the indole proton of Trp36 in the U_{exch} state than that observed for the F_{exch} state, consistent with the model in which Trp36 indole belongs to a non-native cluster. Thus, although the U_{exch} state may be described as a dynamically interconverting ensemble of conformers, there appears to be significant asymmetry in the environment of the indole group and the six-membered ring or backbone of Trp36. This implied lack of averaging of a side chain position is in contrast to the general view of fluctuating side chains within disordered states.

Many proteins possess significant regions of intrinsic disorder (*1*). Interestingly, a high proportion of these proteins are involved in signaling (*2*) and cell cycle processes. It is currently believed that disordered regions facilitate complex regulation by mediating protein interactions in a highly adaptable manner. The extended state also affords the advantage of a greater interaction surface. To better understand the role of protein disorder, structural or topological information about disordered states of proteins, ideally under nondenaturing conditions, is critical. In NMR experiments, such information may come from the observation of nuclear Overhauser effects (NOEs) (*3*), paramagnetic relaxation enhancement (PRE) (*4*, *5*), residual dipolar couplings (RDCs) (*6*, *7*), chemical shift deviations from random coil values (*8*−*11*), or scalar couplings (*12*). Another useful structural tool for the study of disordered proteins is the measurement of solvent exposure. Normally, contact with the solvent in disordered systems can be investigated by CLEANEX-type hydrogen exchange between solvent and protein protons (*13*, *14*) or by the addition of contrast agents to the solvent and the subsequent study of changes in the chemical shifts or relaxation rates of resonances associated with solvent-exposed residues on the protein surface (*15*, *16*). Here we define contrast agent to mean any additive which affects a change in line width, chemical shift, or T_1 as a function of local environment, and as such, a contrast agent may be paramagnetic or a simple isotope as in the case of D_2O which gives rise to measurable shifts for solvent-exposed ^{19}F labels. We utilize ^{19}F and ^{1}H NMR and compare the effects of dissolved oxygen and more traditional additives to investigate solvent exposure and hydrophobicity at various sites belonging to the tryptophan residue involved in a non-native cluster in the unfolded state of a marginally stable protein.

The isolated N-terminal SH3 domain of the *Drosophila* signal transduction protein Drk (i.e., the drkN SH3 domain) is a highly useful model protein for the study of structure within the disordered state. Under nondenaturing conditions, the protein exists in slow exchange between a folded (F_{exch}) and a highly populated compact unfolded (U_{exch}) state (*17*, *18*). Like other SH3 domains, the folded state forms a β-sandwich as shown in Figure 1 (PDB entry 2A36) (*19*).

† The work was supported by grants from the Petroleum Research Council (R.S.P.), NSERC (R.S.P. and J.D.F.-K.), and the Canadian Institutes of Health Research (J.D.F.-K.).

* To whom correspondence should be addressed: Chemistry, University of Toronto, UTM, 3359 Mississauga Rd. North, Mississauga, Ontario, Canada L5L 1C6. E-mail: sprosser@utm.utoronto.ca.

‡ Department of Chemistry, University of Toronto.

§ Hospital for Sick Children.

|| Department of Biochemistry, University of Toronto.

10.1021/bi061389r CCC: $33.50
Published on Web 11/03/2006

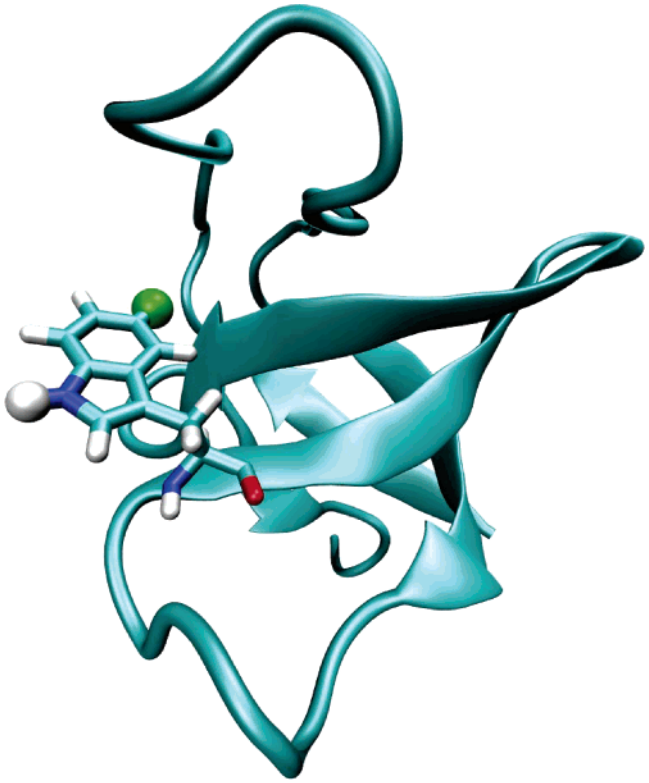

FIGURE 1: Ribbon diagram of the drkN SH3 domain illustrating the regions of major secondary structure in the F_{exch} state, along with the location of the fluorine atom (green sphere) and indole proton (white sphere) in Trp36.

The U_{exch} state can be described as an ensemble of rapidly interconverting conformers, some of which possess long-range contacts and residual structure (*3*). Small-angle X-ray scattering and NMR diffusion measurements suggest that the U_{exch} state is relatively compact, possessing an average radius of gyration ~10% larger than that of the F_{exch} state, compared to a 60% larger radius expected for a random coil structure (*20*).

In the drkN SH3 domain U_{exch} state, Trp36 appears to play a key structural role. Tryptophan is involved in a non-native cluster with non-native NOE contacts observed between aromatic residues Trp36 and Tyr37 and various residues within a non-native helix which extends from amino acids 18 to 28 (*3*, *21*−*23*). Thr22 also appears to play a role in stabilizing the interaction between the non-native helix and the two aromatic residues, as evidenced by mutational analysis (*24*). NOESY experiments revealed at least three long-range amide NOEs ($\geq i$, $i + 5$) to the indole group of Trp36 in the U_{exch} state in a perdeuterated version of drkN SH3 (*3*) and a number of medium- and long-range methyl NOE contacts to the indole proton of Trp36 in a sample of selectively protonated aromatic and δ-methyl-protonated Ile and Leu residues in otherwise perdeuterated drkN SH3 (*19*). This notion of significant clustering in the vicinity of Trp36 in the U_{exch} state is corroborated by near-UV CD studies, obtained by deconvoluting signal from U_{exch} and folded states, which revealed that Trp36 is involved to the same extent in inter-residue contact as in the F_{exch} state (*22*). In addition, stopped-flow fluorescence data also suggested the Trp ring is more buried in the unfolded state than in the folded state, where it lies on the binding surface (*22*). These measurements (i.e., intramolecular NOEs, fluorescence, and near-UV CD) are consistent with dynamic hydrophobic clustering or structure associated with hydrophobic residues seen in other unfolded and disordered states. Tryptophan residues are routinely involved in such clusters (*25*). In the case of the stabilizing Trp cage motif, there is a long-range hydrogen bond between the tryptophan indole proton and a backbone carbonyl group of another residue (*26*).

Greater detail of clustering and solvent protection in the U_{exch} state may be obtained from NH proton-exchange studies. In this case, CLEANEX experiments, tailored to detect only amide or indole protons in rapid exchange with the solvent (*14*), revealed that while the majority of backbone amide protons in the unfolded state ensemble appear to be unprotected from exchange with solvent, the indole of Trp36 is at least 90% buried in the unfolded state with backbone amides of nearby Asn35 and Arg38 residues also partially protected (*22*). The absence of significant protection for most backbone amides points toward an ensemble of rapidly interconverting conformers in the U_{exch} state with no stable hydrogen-bonded elements of secondary structure. Remarkably, within this dynamic ensemble, a prominent asymmetry for Trp36 persists, where the backbone amide exhibits relatively little solvent protection and the indole proton appears to be significantly protected. The use of a fluorine probe on the six-membered ring of Trp36 provides the possibility of examining solvent protection at another site on the side chain, thereby allowing closer study of this asymmetry.

Though the Trp36 indole group is clearly involved in non-native inter-residue contacts, it is difficult to estimate the actual fraction of rapidly interconverting conformers in the U_{exch} ensemble which possess features representative of the non-native hydrophobic cluster, based primarily on NOE data. Distance constraints based on NOEs depend on the spectral density term, which explicitly "weights" a given NOE according to the time scale and amplitude of local motion. For example, in the simplest model where the motion is parametrized by a single reorientational correlation time, τ_c, the cross relaxation rate, σ, associated with the NOE between two homonuclear $S = {}^1/_2$ species of gyromagnetic ratio γ and separated by distance r is given by

$$\sigma = \frac{\gamma^4\hbar^2}{10[\mu_0/(4\pi)]^2}\left\langle\frac{1}{r^6}\right\rangle\left[\frac{6/\tau_c}{(1+4\omega^2\tau_c{}^2)} - \tau_c\right] \qquad (1)$$

where $\hbar$ and μ_0 are well-known constants (*27*). Thus, an ensemble of rapidly interconverting conformers may give rise to an average distance term, $\langle 1/r^6\rangle$, where the relative weighting depends explicitly on dynamics or differences in dynamics within the ensemble. In contrast, soluble relaxation agents whose electronic relaxation times are sufficiently short, as in the case of O_2 and Ni(II), are not affected by dynamic processes or interconversion between conformers and reflect a simple population-weighted average property of the ensemble. Therefore, these approaches can serve as an ideal complement to NOE measurements for purposes of assessing solvent exposure and local hydrophobicity of the key tryptophan residue believed to be involved in this non-native hydrophobic cluster. Furthermore, since CLEANEX-type experiments focus on fast proton exchange with NH

groups, it is advantageous to consider methods in which it is possible to observe a greater range of solvent exposure and/or protection, while it is also desirable to determine the hydrophobicity of the local environment to ascertain if a specific region is protected due to hydrophobic clustering or local hydrogen bonding.

Fluorine NMR has several distinct advantages in studies of solvent exposure. In the absence of contrast agents, T_1 is generally shorter for buried than solvent-exposed ^{19}F nuclei (*28*). ^{19}F NMR spectra of specifically fluorinated proteins often reveal dramatic changes in chemical shifts and line shapes between folded and unfolded or chemically denaturated states (*29*−*31*). However, since interpretation of such chemical shift changes in terms of structure may be difficult (*29*), paramagnetic additives offer a potential advantage in terms of quantitative interpretation of the degree of solvent exposure and, consequently, of protein folding and unfolding events. Soluble paramagnetic contrast agents such as Dy^{3+}:EDTA, Gd^{3+}:EDTA, or nitroxide spin-labels generally give rise to large ^{19}F NMR chemical shift perturbations and/or enhancement of both spin−spin and spin−lattice relaxation rates (*32*, *33*). Relaxation enhancement arises partly from the fact that the ^{19}F nucleus has a high gyromagnetic ratio and is thus strongly relaxed by paramagnetic species through dipolar mechanisms. Chemical shift effects arise from the lone-pair valence electrons which participate in nonbonded interactions, making the fluorine nuclear spin sensitive to changes in van der Waals contacts, electrostatic fields, and hydrogen bonding (*34*). Even the substitution of D_2O for H_2O is known to yield a 0.25 ppm chemical shift perturbation in ^{19}F NMR applications of solvent-exposed residues (*28*, *35*, *36*), while the addition of paramagnetic species such as dissolved oxygen may give shifts as large as 5 ppm, in addition to causing large relaxation rate enhancements at partial pressures of ≥20 atm (*37*−*39*).

In general, chemical shift perturbations or relaxation enhancements from contrast agents may result from both the degree of solvent exposure and possible local partitioning of the contrast agent. For example, paramagnetic additives such as TEMPO are known to preferentially interact with aromatic residues (*40*), while dissolved oxygen is expected to partition into accessible hydrophobic or disordered pockets. As discussed below, it is possible to distinguish between steric effects (i.e., solvent-exposed surface area) and hydrophobic partitioning effects by a judicious choice of contrast agents whose sizes are comparable but where one species is hydrophobic and the other hydrophilic. In the context of ^{19}F NMR, water and oxygen are an ideal choice since H_2O/D_2O solvent isotope effects can be easily measured as are paramagnetic effects of dissolved oxygen. Similarly, paramagnetic rates from dissolved oxygen and NOE effects from water are easily observed in ^{1}H NMR applications. Solvent exposure and hydrophobicity are important aspects of loosely packed hydrophobic clusters and disordered systems in general. Thus, it is important to develop an experimental protocol to distinguish the two effects. In this paper, we examine contact with both water and dissolved oxygen, using ^{19}F NMR and ^{1}H NMR to distinguish hydrophobic effects and solvent exposure. The results reveal detailed site specific information demonstrating that Trp36 is clustered in the U_{exch} state such that the indole group is protected from solvent while the 5 position of the aromatic ring is completely exposed to the solvent. Thus, the contrast experiments described provide localized information which highlights the dramatic asymmetry in environment associated with Trp36 in the U_{exch} state.

MATERIALS AND METHODS

Sample Preparation. A plasmid encoding the isolated WT drkN SH3 domain, residues 1−59 of Drk (*17*), under the control of the T7 promoter, was transfected into *Escherichia coli* HMS 174 cells. The expression of the ^{15}N-labeled protein was induced for 1 h at an OD_{600} of 0.6 by addition of 250 mg/L IPTG to bacterial growths at 37 °C in M9 minimal medium, supplemented with 0.3% D-glucose, 0.1% $^{15}NH_4Cl$, 100 mg/L ampicillin, 10 mg/L thiamine, 10 mg/L biotin, 1 mM $MgSO_4$, and 1 mM $CaCl_2$. To introduce fluorotryptophan into drkN, ^{19}F-labeled 5-fluoro-L,D-Trp was added to the bacterial culture at a concentration of 600 mg/L, 1 h prior to induction. Note that the literature recommends addition of only 60 mg/L, and the 10-fold excess that was utilized was very likely to be unnecessary. Growth was halted 1 h after induction, rather than 3 h. Cells were lysed by sonication in 50 mM Tris, 2 mM EDTA, 5 mM benzamidine HCl, and 7 mM β-mercaptoethanol. The drkN SH3 domain was purified on a DE 52 ion-exchange column with a linear gradient of NaCl (from 0 to 1 M) followed by purification on a Superdex 75 gel filtration column in 0.15 M NaCl, 50 mM Tris, 2 mM EDTA, 5 mM benzamidine HCl, and 7 mM β-mercaptoethanol, and then a Mono Q ion-exchange column with a linear gradient of NaCl (from 0 to 0.3 M). All purification steps were performed at 4 °C.

NMR Experiments. The protein concentration was approximately 0.2 mM in 50 mM phosphate buffer (pH 6.0). A 350 μL sample volume was deemed sufficient for shimming purposes, using a 5 mm outside diameter, 3 mm inside diameter sapphire NMR sample tube (Saint Gobain-Saphikon Crystals, Milford, NH) designed to tolerate pressures as high as 270 bar. To measure effects of dissolved oxygen, the sample was first equilibrated at 5 °C outside the magnet at an oxygen partial pressure of 40 atm for 2 days and then equilibrated overnight in the magnet at the desired partial pressure of 20 atm. Using open Swagelok connections (Swagelok, Solon, OH) to a pressurized oxygen supply, it was possible to maintain the pressure during the entire course of the NMR experiment. Control experiments on free, dissolved 5F-Trp were also performed both with and without oxygen. To reproduce oxygen concentrations, we relied on the measurement of the ^{1}H T_1 of water (i.e., 0.16 s for the fluorotrptophan drkN SH3 sample under an oxygen partial pressure of 20 atm and 0.154 s for the free 5F-Trp amino acid sample under an oxygen partial pressure of 20 atm). Upon completion of oxygen experiments, the sample was degassed by first being transferred to a 1.5 mL microfuge tube resting on an ice bath, after which it was slowly stirred using a sterile needle tip which precipitated the bubbling of oxygen. The sample was then left for 24 h in a nitrogen environment to allow for residual degassing. To exchange H_2O for D_2O buffer, a 0.5 mL centrifugal concentrator with a molecular mass cutoff of 3 kDa was used. A modest amount of protein (30%) was lost upon solvent exchange and transfer back to the original sapphire NMR tube, resulting in a need for greater signal averaging in the D_2O sample.

^{1}H and ^{19}F one-dimensional NMR experiments and ^{1}H,^{15}N gradient-selected HSQC two-dimensional experiments were performed at 5 °C on a 600 MHz Varian Inova spectrometer, using a standard HCN triple-resonance single-gradient solution NMR probe, in which the high-frequency channel could be tuned to either ^{19}F or ^{1}H. Sixteen scans and 80 increments spanning 1800 Hz in the indirect dimension were used to obtain the HSQC spectrum, while at least 256 scans were used to obtain the ^{19}F NMR spectrum. Note that backbone amide assignments of the ^{19}F-labeled drk SH3 domain were obtained on the basis of their proximity to previously assigned resonances in the unfluorinated protein. ^{1}H indole T_1 measurements were carried out via a standard inversion recovery sequence where the solvent signal was suppressed by a WATERGATE filter sequence (*41*); since the 5F-Trp was not ^{15}N-enriched, the ^{1}H indole signals from the U_{exch} and F_{exch} states were detected directly. The measurement of ^{19}F spin−lattice relaxation times was accomplished by an inversion recovery sequence (i.e., 180°−τ−90°) using a total of eight τ values, logarithmically spaced between 10 ms and 5 s (ambient sample) or 1 ms and 1 s (oxygenated sample). The repetition time was adjusted to either 6.5 or 1.5 s for the ambient or oxygenated samples, respectively. Two Hahn echo refocusing pulses, spaced by 350 μs, were appended to all ^{19}F NMR sequences to help filter out the background ^{19}F signal from the probe. In a separate (unfluorinated) sample of the drkN SH3 domain, prepared as described previously (*3*), contact of water with the tryptophan indole and backbone amide protons was assessed using an ePHOGSY NOE experiment (*42*, *43*) with mixing times ranging from 50 ms to 2 s. The slope associated with the initial buildup of NOE signal could be determined and was used to estimate the NOE.

RESULTS

Effect of Fluorination of Trp36. Figure 2A compares the ^{1}H,^{15}N HSQC NMR spectrum of the ^{15}N-enriched drkN SH3 domain (black contours) with that of the 5F-Trp substituted form (red contours). Note that there is no detectable ^{15}NH tryptophan signal from the fluorotryptophan substituted species, suggesting that the level of incorporation of [^{19}F]-Trp was at least 98%, based on the signal-to-noise ratio in the HSQC spectrum. The two spectra of fluoro-drkN SH3 and drkN SH3 domains overlap with modest differences in chemical shifts, suggesting that even a single fluorine atom substitution may have subtle effects on conformation in the case of marginally stable and disordered proteins. The similarity in the HSQC spectra suggests that the conformations of the fluorinated and unfluorinated proteins are similar in both states. However, without additional experiments including a detailed comparison of ^{1}H−^{1}H and ^{1}H−^{19}F NOEs, one cannot rule out minor differences in conformation or dynamics introduced by the fluorine atom. Figure 2B presents the ^{15}N,^{1}H chemical shift deviations resulting from the substitution of 5F-Trp for both the F_{exch} (black bars) and U_{exch} states (white bars). Note that the chemical shift deviations are greater for the F_{exch} state, which is perhaps not surprising since the folded state is more compact, leading to closer distances between protons and the fluorine atom. It is also clear that the shift perturbation profiles show little resemblance for each of the two states, which emphasizes the distinctly different environment that Trp36 occupies in

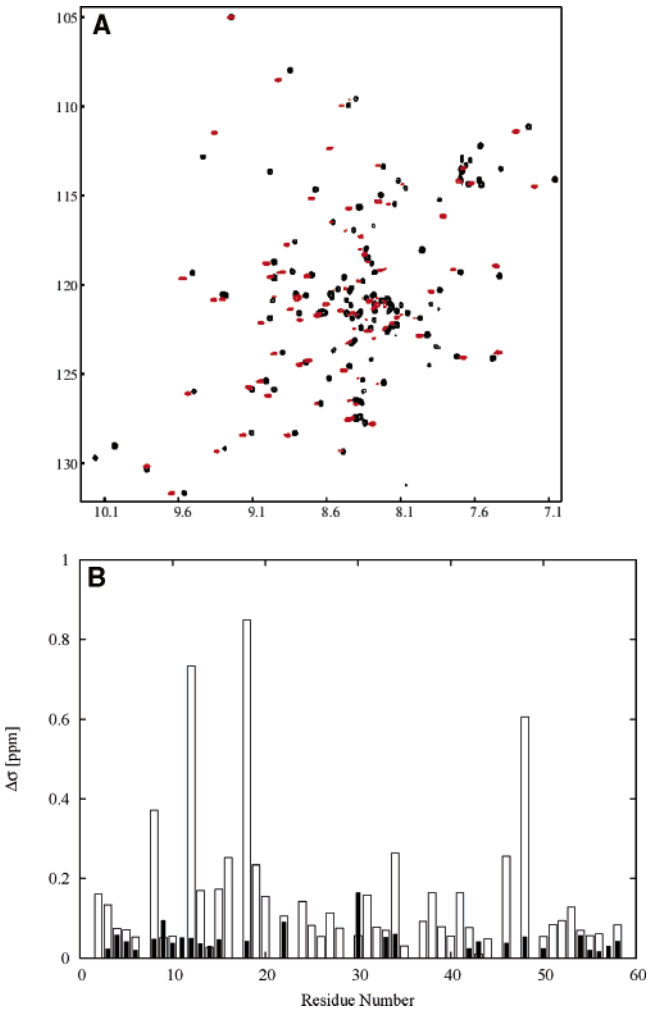

FIGURE 2: (A) ^{1}H,^{15}N HSQC NMR spectrum of the ^{15}N-enriched drkN SH3 domain (black) overlaid with the equivalent spectrum of the drkN SH3 domain in which Trp36 is replaced with 5F-Trp (red). Both spectra were acquired at 5 °C. (B) A histogram indicating the weighted average of chemical shift perturbations resulting from replacing Trp36 with 5F-Trp36 for both the F_{exch} state (white bars) and the U_{exch} state (black bars) of the drkN SH3 domain. Shift perturbations are calculated as a weighted average of shifts in both the ^{1}H and ^{15}N dimensions [$\Delta\sigma = \sqrt{|\Delta\sigma(^1\mathrm{H})|^2+0.2|\Delta\sigma(^{15}\mathrm{N})|^2}$].

the F_{exch} and U_{exch} states. There is a substantial shift in the equilibrium toward the F_{exch} state upon substitution of 5F-Trp36. The equilibrium between the F_{exch} and U_{exch} states of drkN is a very delicate one (*19*); the free energy barrier has been previously estimated to be 0.4 kcal/mol (*44*). The T22G mutation shifts the equilibrium dramatically toward the F_{exch} state, due partially to the disruption of residual non-native helical structure in the U_{exch} ensemble and an increase in its free energy (*24*). Moreover, it has proven very difficult to mutate Trp36 to other residues without significantly altering the stability of the protein (M. Tollinger and J. D. Forman-Kay, unpublished results). The dramatic stabilization of the folded state by a single fluorine atom is not unprecedented; the substitution of Trp187 with the 5-fluorinated version resulted in a stabilization of human recombinant annexin V (*45*). The ^{19}F NMR spectrum of the 5F-Trp substituted drkN SH3 domain, obtained under conditions identical to those of the unfluorinated drkN SH3 domain, is shown in Figure

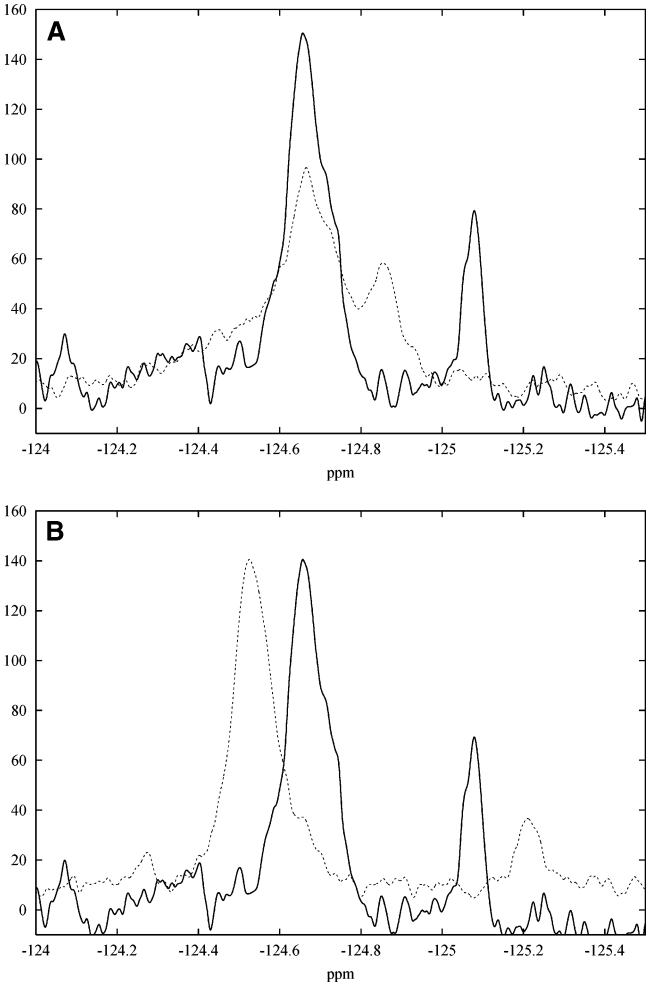

FIGURE 3: (A) ^{19}F NMR spectra of the 5F-Trp-substituted drkN SH3 domain obtained at 5 °C. Solid and dashed lines represent the spectra under unoxygenated and oxygenated conditions, respectively. (B) ^{19}F NMR spectra of the 5F-Trp-substituted drkN SH3 domain obtained at 5 °C. The solid line represents the spectrum of the drkN SH3 domain in a 90/10 H_2O/D_2O mixture, while the dashed line represents the spectrum after exchanging the buffer with a 10/90 H_2O/D_2O mixture.

3A (solid line). Definitive assignments could be made to the F_{exch} and U_{exch} states in the ^{19}F NMR spectrum, based on the ratio of areas of the two peaks [i.e., area(F_{exch})/area(U_{exch}) = 3.16 at 5 °C] since the ratio of volume integrals from previously assigned resonances in the HSQC spectrum associated with the two states clearly indicated that the ratio of conformers was 3.0. Note that the line widths associated with the F_{exch} and U_{exch} resonances are approximately 63 and 25 Hz, respectively, while the spin−lattice relaxation times of each of the two conformers are 0.50 ± 0.03 and 0.72 ± 0.09 s, respectively.

Assessing Solvent Exposure by Dissolved Oxygen. The addition of dissolved oxygen has a significant effect on the U_{exch} state where a shift of +0.217 ± 0.001 ppm is observed, while the F_{exch} state effectively does not shift within the above uncertainty of 0.001 ppm as shown by the ^{19}F NMR spectra in Figure 3A. To interpret the paramagnetic shifts with respect to solvent exposure, we consider first the shift perturbation of +0.169 ppm experienced by 5F-Trp, free, dissolved in water under conditions identical to those of the protein. The resulting ratios of the paramagnetic shifts of 5F-Trp in the drkN SH3 domain to those of the free (fully exposed) residue are 1.284 and 0.00 for the U_{exch} and F_{exch} states, respectively. Since the oxygen-induced shift associated with the U_{exch} state is even greater than that observed for free 5F-Trp, it is tempting to conclude that the 5-fluoro position of Trp36 is thus fully exposed in the U_{exch} state. However, the contrast effect of dissolved oxygen may result from two effects: (1) the degree of solvent exposure and (2) preferential partitioning of oxygen in the vicinity of the probe nucleus, resulting in shifts greater than that experienced in bulk solvent. The latter effect could arise from a local cavitation effect (*46*) and/or from the hydrophobic character in the vicinity of the probe nucleus. This is not unexpected since Trp36 is proposed to participate in a non-native hydrophobic cluster, which is presumably dynamic or sufficiently loosely packed to facilitate oxygen accessibility. It should be possible to distinguish hydrophobic partitioning effects from solvent exposure by performing additional measurements which utilize hydrophilic contrast agents as discussed below. Accessibility to dissolved oxygen is also detected by ^{19}F NMR spin−lattice relaxation measurements, and results of these experiments are given in Table 1. After the paramagnetic rates observed for both the F_{exch} and U_{exch} states have been divided by the paramagnetic rate observed for free 5F-Trp, under identical conditions, the enhancement ratios [i.e., $R_1^P \equiv R_1^P$(5FTrp−drkN)/R_1^P(5FTrp−free)] are 1.70 and 0.65 for the U_{exch} and F_{exch} states, respectively. In this case, the paramagnetic enhancement ratio observed for the U_{exch} state is even higher than that observed from chemical shift perturbations. Thus, the 5 position of Trp36 experiences a significant degree of solvent exposure and/or local partitioning of O_2 in the U_{exch} state.

Assessing Solvent Exposure by the Solvent Isotope Effect. An established way of considering solvent exposure is simply to replace H_2O with D_2O, since ^{19}F NMR resonances of exposed probes are known to shift by as much as 0.25 ppm under such circumstances (*28*). Figure 3B compares the ^{19}F NMR spectrum of the 5-fluoro-substituted drkN SH3 domain at 5 °C in an approximately 10/90 H_2O/D_2O mixture (dashed line) to the original spectrum in a 90/10 H_2O/D_2O mixture (solid line). In this case, there is a downfield shift observed for the ^{19}F resonance associated with the F_{exch} state (i.e., 0.146 ppm), while an upfield shift (i.e., −0.132 ppm) is observed for the resonance associated with the U_{exch} state, which is similar to the shift of −0.109 ppm observed for free, dissolved 5F-Trp, under identical conditions. If solvent exposure were the only consideration, we would expect an upfield shift when H_2O was replaced with D_2O. Although there are numerous explanations for the anomalous solvent isotope shift associated with the F_{exch} resonance, it may originate from a specific interaction of fluorine with a bound water molecule and/or with the protein itself. This is also suggested by the earlier observation that the equilibrium changed dramatically in favor of the F_{exch} state upon substitution of a hydrogen for a fluorine atom at the 5 position, while the paramagnetic shift from dissolved oxygen was noted to be zero. Fluorine is well-known to act as a weak hydrogen bond acceptor (*45*), and in our case, it significantly stabilizes the folded conformation.

The equilibrium between the F_{exch} and U_{exch} states also changes dramatically upon substitution of D_2O, as seen in Figure 3B, where the ratio of conformers in the F_{exch} to U_{exch}

Table 1: Results of T_1 Measurements in 90% H_2O/10% D_2O and 10% H_2O/90% D_2O Mixtures in Addition to Solvent Isotope Shifts and Paramagnetic Shifts and Rates Resulting from Dissolved Oxygen for the 5-Fluoro Position and the Indole Proton

	T_1 (s) in 90% H_2O	T_1 (s) in 100% D_2O	$R_1^p(O_2)$ (Hz)	$\Delta\delta_{O_2}$ (ppm)	$\Delta\delta(D_2O-H_2O)$ (ppm)
^{19}F-labeled F_{exch}	0.50 ± 0.03	1.98 ± 0.01	2.18	0 ± 0.015	+0.146
^{19}F-labeled U_{exch}	0.72 ± 0.09	5.61 ± 0.01	5.61	0.217 ± 0.015	−0.132
^{19}F (free Trp)	1.168	1.139 ± 0.005	3.34	0.169 ± 0.015	−0.109
^{1}H indole F_{exch}	1.56 ± 0.01	NA[a]	4.74	NA[a]	NA[a]
^{1}H indole U_{exch}	0.979 ± 0.005	NA[a]	4.0	NA[a]	NA[a]

[a] Not available.

state has roughly doubled. Water undoubtedly participates in a multitude of electrostatic and hydrogen bonding interactions with the protein. In either case, the magnitude of the free energy associated with such interactions is lowered upon introduction of D_2O, and the equilibrium shifts toward the state involving fewer bound waters (i.e., F_{exch}). However, the isotope effect is at least as dramatic in the unfluorinated drkN SH3 domain where the change in the ratio of F_{exch} to U_{exch} conformers is more than a factor of 2, suggesting that the Gibbs free energy of unfolding is not substantially changed by the introduction of the fluorine atom.

The above solvent-induced shift results may also be normalized by first measuring the chemical shift perturbation when H_2O is replaced with D_2O for free 5F-Trp. The resulting ratio of chemical shift change for the intact protein to that of the free amino acid is 1.21 for the U_{exch} state. Thus, the 5 position of Trp36 appears to be completely exposed to solvent in the U_{exch} state to the extent that the solvent exposure even surpasses that observed for free 5F-Trp. One plausible explanation is that the density of water in the vicinity of the 5-fluoro position of the protein is higher than that for the bulk solvent which is not unprecedented in studies of protein surfaces (*47*−*50*). Prior studies have reported that in comparison to the free amino acids, water is often more structured out to as many as two hydration shells, particularly in the case of polar side chains (*49*).

^{19}F NMR spin−lattice relaxation rates and line widths are also of some use in confirming the degree of packing and thus, solvent exposure, in the absence of oxygen. In deuterated solvent and assuming that dipolar relaxation dominates, the relaxation rate is known to be a useful reporter of the weighted density of surrounding protons (i.e., $\sum r^{-6}$). In D_2O, the ^{19}F NMR spin−lattice relaxation rate of the 5-fluoro probe in the U_{exch} state is 0.178 Hz which is significantly smaller than that of the folded state (0.505 Hz). This may be compared with the relaxation rate associated with free 5F-Trp which is observed to be 0.88 Hz. Thus, barring gross differences in local hydrophobicity and oxygen partitioning, we find the solvent isotope shifts, effects of dissolved O_2, and ambient spin−lattice relaxation rates all suggest that the 5F position is significantly more exposed to solvent in the U_{exch} state than in the F_{exch} state.

Distinguishing between Steric Effects and Partitioning Effects with Contrast Agents. Contrast agents are of tremendous use in the evaluation of steric effects or solvent exposure. However, we must consider the extent to which the contrast agent associates with specific residues or groups or even partitions into the protein, particularly in cases where the protein is unfolded or partially unfolded. To distinguish between steric and partitioning effects, we can make use of contrast agents of similar size, whose hydrophobicities are dramatically different (*51*). In this case, we compare the contrast effects from water and oxygen. Focusing on variables relevant to this study, in the weak collision limit we may express the chemical shift perturbation, $\Delta\delta_{O_2}$, due to contact with oxygen as (*52*)

$$\Delta\delta_{O_2} = k\langle\Omega\rangle\alpha\langle[O_2]\rangle_{local} \quad (2)$$

where k represents a proportionality constant, $\langle\Omega\rangle$ is a collisionally accessible surface area, α represents a polarization or spin delocalization term, and $\langle[O_2]\rangle_{local}$ signifies the local oxygen concentration. If we further consider the normalized equivalent of the above chemical shift perturbation, $\Delta\delta^*_{O_2}$, in which we divide the measured chemical shift perturbation by that observed for free, dissolved 5F-Trp, then we expect the dominant terms to simply involve the ratio of accessible surface areas and the ratio of local oxygen concentrations such that

$$\Delta\delta^*_{O_2} \equiv \frac{\Delta\delta_{O_2(5FTrp-drk)}}{\Delta\delta_{O_2(5FTrp-free)}} = \frac{\langle\Omega\rangle_{O_2(5FTrp-drk)}[O_2]_{local}}{\langle\Omega\rangle_{O_2(5FTrp-free)}[O_2]_{bulk}} \quad (3)$$

Note that the ratio of surface areas should certainly be less than unity, suggesting that the overall normalized shift can be greater than unity only if the region in the vicinity of the probe is hydrophobic. In our case, measurements of the oxygen-induced shift perturbations of the 5F-Trp probe in the U_{exch} state and of free, dissolved 5F-Trp, under identical conditions, reveal that $\Delta\delta^*_{O_2} = 1.284$, suggesting $[O_2]_{local}/[O_2]_{bulk} \geq 1.284$. We may similarly define the normalized version of the chemical shift perturbation due to the solvent isotope effect as

$$\Delta\delta^*_{H_2O} \equiv \frac{\Delta\delta_{D_2O-H_2O(5FTrp-drk)}}{\Delta\delta_{D_2O-H_2O(5FTrp-free)}} = \frac{\langle\Omega\rangle_{H_2O(5FTrp-drk)}[H_2O]_{local}}{\langle\Omega\rangle_{H_2O(5FTrp-free)}[H_2O]_{bulk}} \quad (4)$$

Although this is not of paramagnetic origin, we nevertheless expect the normalized version of the chemical shift perturbation arising from substitution of H_2O for D_2O to depend on a similar product of ratios as above. Again, solvent isotope shift effects of both free 5F-Trp and the 5F-Trp probe from the U_{exch} state of the drkN SH3 domain reveal that $\Delta\delta^*_{H_2O} = 1.21$, whereupon we conclude that $[H_2O]_{local}/[H_2O]_{bulk} \geq 1.21$. Assuming that the collisional accessibilities of water and oxygen are similar, the ratio of accessible surface areas in both eqs 3 and 4 will be identical. If we make this approximation, we may then consider the ratio of the above normalized shifts which provides an estimate of

the partitioning potential of oxygen and water and, thus, hydrophobicity, which we express as

$$\frac{\Delta\delta^*_{O_2}}{\Delta\delta^*_{H_2O}} = \frac{[O_2]_{local}/[O_2]_{bulk}}{[H_2O]_{local}/[H_2O]_{bulk}} \quad (5)$$

The above measurements of $\Delta\delta^*_{O_2}$ and $\Delta\delta^*_{H_2O}$ reveal that the relative partitioning term is on the order of $[\Delta\delta^*_{O_2}]/[\Delta\delta^*_{H_2O}] = 1.06$. Thus, we conclude that the 5-fluoro position of Trp36 is nearly completely solvent exposed in the U_{exch} state and only marginally hydrophobic.

^{1}H NMR Studies of Solvent Exposure to the Trp36 Indole. A considerable body of literature suggests that the indole group of Trp36 serves as a key contact point associated with the non-native hydrophobic cluster (*3*, *19*, *21*, *22*). To further investigate the role of Trp36 in establishing non-native contacts in the U_{exch} state, the extent of solvent exposure on the indole proton of Trp36 has therefore been measured by NOE effects from water and by T_1 relaxation effects from dissolved oxygen. In contrast to the 5-fluoro position, which appeared to be completely exposed to the solvent {i.e., $[R_1^P(O_2,U_{exch})]/[R_1^P(O_2,F_{exch})] = 2.6$}, the indole group appears slightly less exposed in the unfolded state than in the folded state {$[R_1^P(O_2,U_{exch})]/[R_1^P(O_2,F_{exch})] = 0.84$}. Prior CLEANEX experiments corroborate this notion of solvent protection at the indole group of Trp36 in the U_{exch} state and reveal the nearly complete absence of fast chemical exchange with water at the indole group of Trp36. However, water NOESY experiments which were performed via an ePHOGSY pulse sequence (*53*) revealed somewhat greater contact with water in the vicinity of the indole protons in the U_{exch} state than in the F_{exch} state. In this case, the NOE intensities were determined from the initial slope associated with the change in peak intensity with mixing time. Whereas the backbone amide proton exhibited a 3-fold greater NOE rate with respect to water in the U_{exch} state than in the F_{exch} state, the water NOE rates, σ^{NOE}, to the indoles were comparable {$[\sigma^{NOE}(H_2O,U_{exch})]/[\sigma^{NOE}(H_2O,F_{exch})] = 1.17$}. While CLEANEX experiments are designed to detect fast exchanging water, the above water NOE measurements are indicative of bound water or possibly a relayed effect from an exchangeable proton on a nearby side chain.

DISCUSSION

The sole tryptophan in the drkN SH3 domain has been of great interest due to considerable NOE evidence (*3*) which shows long-range contacts from Trp36 in the U_{exch} state to a non-native helix corresponding to residues in the diverging turn region of the folded state and hydrogen-exchange protection of the indole proton (*22*). To investigate the degree of solvent exposure and hydrophobicity associated with another position in the Trp36 ring, we have made use of an isotopic fluorine probe at the 5 position of the tryptophan residue. Specifically, hydrophobicity was assessed by comparing the ratio of the normalized shift arising from dissolved oxygen to that associated with the solvent isotope effect. In principle, one can conceive of a similar approach with respect to ratios of normalized relaxation rates, and such an approach was recently taken in a ^{1}H solution NMR study of a membrane protein where a ratio was derived on the basis of a paramagnetic rate associated with dissolved oxygen and a rate of transfer of water magnetization (*54*). One might also conceive of utilizing a ratio of paramagnetic rates arising from dissolved oxygen and a chelated Ni(II) species, since both are ideal paramagnetic probes for NMR because of their short electronic spin relaxation times.

On the basis of ^{1}H NMR studies of the indole protons and ^{19}F NMR studies of the fluorine label at the 5 position, Trp36 appears to be situated in the protein in the U_{exch} state such that the 5 position of the Trp ring is significantly exposed to the solvent while the indole proton is less exposed. The fluorine probe allowed for the sensitive study of solvent exposure in both the F_{exch} and U_{exch} states. ^{19}F NMR chemical shift perturbations and T_1 relaxation enhancement from dissolved oxygen reveal that the 5 position of Trp36 is largely exposed to the solvent in the U_{exch} state while slightly more protected in the F_{exch} state. Normalized paramagnetic relaxation rates from dissolved oxygen are 0.65 and 1.70 for the F_{exch} and U_{exch} states, respectively. Moreover, contrast experiments using both a hydrophobic probe (dissolved oxygen) and a hydrophilic probe (water) allowed us to separately evaluate the relative partitioning of oxygen versus water in the vicinity of Trp36 and, in so doing, assess the hydrophobicity. The results suggest that the region in the vicinity of the 5-fluoro position of Trp36 is not hydrophobic and that slightly increased accessibility to water and oxygen occurs. Although there is a precedent for the observation of higher water densities at the protein surface, we can only speculate about the origin of slightly stronger effects of oxygen at the identical site. Prior studies have observed that, in comparison to the free amino acids, the mean residence times of water vary dramatically over protein surfaces (*55*, *56*). It is also conceivable that the average oxygen-bound lifetime is increased in the vicinity of the fluorine atom of Trp36, giving rise to a greater paramagnetic shift effect than that seen in the free amino acid.

Prior NH-exchange experiments on the indole and backbone amide protons of Trp36 suggest a stark asymmetry in terms of solvent protection for Trp36 in the U_{exch} state. Subsequent contrast experiments at the 5 position and on the indole proton of Trp36 confirm this asymmetry and suggest that only the indole proton of the five-membered ring is strongly protected from solvent. The indole group may exhibit partial protection from dissolved oxygen because it is involved in a hydrogen bond, presumably to a side chain residue such as T22, for which prior NOE contacts have been observed (*3*). However, this cluster around the Trp36 indole may not be primarily hydrophobic as evidenced by the relatively strong water NOE, based on an ePHOGSY experiment (*57*). The lack of a significant peak in CLEANEX-based experiments (*22*) suggests that there is no contact with fast exchanging solvent molecules and that the above water NOE may involve a strongly bound water or a relayed effect from the T22 side chain.

We note that the approach we have taken in separately assessing solvent exposure or steric effects and hydrophobicity has been adopted successfully in the ESR field. Using nitroxide spin-labels to probe protein topology, it was shown that a water soluble contrast agent such as chelated nickel complemented contrast effects from dissolved oxygen and that a ratio of paramagnetic effects from oxygen and nickel served to factor out steric effects and give a measure of

hydrophobic partitioning (*51*). In our ^{19}F NMR studies, we have followed an analogous approach. Here, water and oxygen serve as ideal and complementary contrast agents for the study of solvent exposure and the separation of steric effects from hydrophobic effects. Contrast effects from oxygen are measured through either paramagnetic shifts or T_1 relaxation enhancement, while the effects of water may be directly observed via solvent isotope shifts. Similarly, in the case of the indole proton, we have made use of water NOEs and oxygen-induced relaxation enhancement.

CONCLUSION

Our results highlight a feature of the U_{exch} state of the drkN SH3 domain that contrasts with conventional wisdom regarding the dynamic conformational averaging of disordered proteins. Although prior work pointed toward the role of Trp36 in stabilizing a hydrophobic cluster, it is clear from the oxygen contrast measurements that the indole portion of Trp36 is indeed involved in clustering whereas the opposite side of the tryptophan ring is relatively exposed to solvent. Prior work has also shown that the backbone amide of Trp36 is relatively exposed to the solvent in comparison to the indole proton in the U_{exch} state (*22*). Considering the extent of motion and range of conformers expected in the U_{exch} state, it is surprising that such asymmetry in the region of Trp36 exists for a single residue within the population-weighted average unfolded state ensemble. While prior NH-exchange experiments also suggested significant asymmetry for Trp36 within the U_{exch} state (*22*), these contrast experiments provide stronger comparative data. Furthermore, water NOE measurements suggest that the region in the vicinity of the indole group in the U_{exch} state is not hydrophobic and may be involved in hydrogen bonding. Further experiments to explore the possibility of a hydrogen bond involving the Trp36 indole within the U_{exch} state are currently underway.

REFERENCES

1. Fink, A. L. (2005) Natively unfolded proteins, *Curr. Opin. Struct. Biol. 15*, 35−41.
2. Uversky, V. N., Oldfield, C. J., and Dunker, A. K. (2005) Showing your ID: Intrinsic disorder as an ID for recognition, regulation and cell signaling, *J. Mol. Recognit. 18*, 343−384.
3. Crowhurst, K. A., and Forman-Kay, J. D. (2003) Aromatic and methyl NOES highlight hydrophobic clustering in the unfolded state of an SH3 domain, *Biochemistry 42*, 8687−8695.
4. Gillespie, J. R., and Shortle, D. (1997) Characterization of long-range structure in the denatured state of staphylococcal nuclease. 1. Paramagnetic relaxation enhancement by nitroxide spin labels, *J. Mol. Biol. 268*, 158−169.
5. Gillespie, J. R., and Shortle, D. (1997) Characterization of long-range structure in the denatured state of staphylococcal nuclease. 2. Distance restraints from paramagnetic relaxation and calculation of an ensemble of structures, *J. Mol. Biol. 268*, 170−184.
6. Bernado, P., Bertoncini, C. W., Griesinger, C., Zweckstetter, M., and Blackledge, M. (2005) Defining long-range order and local disorder in native α-synuclein using residual dipolar couplings, *J. Am. Chem. Soc. 127*, 17968−17969.
7. Bernado, P., Blanchard, L., Timmins, P., Marion, D., Ruigrok, R. W. H., and Blackledge, M. (2005) A structural model for unfolded proteins from residual dipolar couplings and small-angle X-ray scattering, *Proc. Natl. Acad. Sci. U.S.A. 102*, 17002−17007.
8. Wishart, D. S., and Sykes, B. D. (1994) Chemical-Shifts as a Tool for Structure Determination, *Methods Enzymol. 239*, 363−392.
9. Fesinmeyer, R. M., Hudson, F. M., Olsen, K. A., White, G. W. N., Euser, A., and Andersen, N. H. (2005) Chemical shifts provide fold populations and register of β hairpins and β sheets, *J. Biomol. NMR 33*, 213−231.
10. Fong, S., Bycroft, M., Clarke, J., and Freund, S. M. V. (1998) Characterisation of urea-denatured states of an immunoglobulin superfamily domain by heteronuclear NMR, *J. Mol. Biol. 278*, 417−429.
11. Neidigh, J. W., Fesinmeyer, R. M., Prickett, K. S., and Andersen, N. H. (2001) Exendin-4 and glucagon-like-peptide-1: NMR structural comparisons in the solution and micelle-associated states, *Biochemistry 40*, 13188−13200.
12. Hennig, M., Bermel, W., Spencer, A., Dobson, C. M., Smith, L. J., and Schwalbe, H. (1999) Side-chain conformations in an unfolded protein: χ_1 distributions in denatured hen lysozyme determined by heteronuclear C-13, N-15 NMR spectroscopy, *J. Mol. Biol. 288*, 705−723.
13. Gemmecker, G., Jahnke, W., and Kessler, H. (1993) Measurement of Fast Proton-Exchange Rates in Isotopically Labeled Compounds, *J. Am. Chem. Soc. 115*, 11620−11621.
14. Hwang, T. L., Mori, S., Shaka, A. J., and vanZijl, P. C. M. (1997) Application of phase-modulated CLEAN chemical EXchange spectroscopy (CLEANEX-PM) to detect water-protein proton exchange and intermolecular NOEs, *J. Am. Chem. Soc. 119*, 6203−6204.
15. Bertini, I., Luchinat, C., and Parigi, G. (2002) Paramagnetic constraints: An aid for quick solution structure determination of paramagnetic metalloproteins, *Concepts Magn. Reson. 14*, 259−286.
16. Bertini, I., and Luchinat, C. (1986) *NMR of Paramagnetic Molecules in Biological Systems*, Benjamin-Cummings, Menlo Park, CA.
17. Zhang, O., and Formankay, J. D. (1995) Structural Characterization of Folded and Unfolded States of an SH3 Domain in Equilibrium in Aqueous Buffer, *Biochemistry 34*, 6784−6794.
18. Zhang, O. W., and FormanKay, J. D. (1997) NMR studies of unfolded states of an SH3 domain in aqueous solution and denaturing conditions, *Biochemistry 36*, 3959−3970.
19. Bezsonova, I., Singer, A., Choy, W. Y., Tollinger, M., and Forman-Kay, J. D. (2005) Structural comparison of the unstable drkN SH3 domain and a stable mutant, *Biochemistry 44*, 15550−15560.
20. Choy, W. Y., Mulder, F. A. A., Crowhurst, K. A., Muhandiram, D. R., Millett, I. S., Doniach, S., Forman-Kay, J. D., and Kay, L. E. (2002) Distribution of molecular size within an unfolded state ensemble using small-angle X-ray scattering and pulse field gradient NMR techniques, *J. Mol. Biol. 316*, 101−112.
21. Mok, Y. K., Kay, C. M., Kay, L. E., and Forman-Kay, J. (1999) NOE data demonstrating a compact unfolded state for an SH3 domain under non-denaturing conditions, *J. Mol. Biol. 289*, 619−638.
22. Crowhurst, K. A., Tollinger, M., and Forman-Kay, J. D. (2002) Cooperative interactions and a non-native buried Trp in the unfolded state of an SH3 domain, *J. Mol. Biol. 322*, 163−178.
23. Mok, Y. K., Kay, C. M., Kay, L. E., and Forman-Kay, J. (2003) NOE data demonstrating a compact unfolded state for an SH3 domain under non-denaturing conditions , *J. Mol. Biol. 329*, 185−187.
24. Mok, Y. K., Elisseeva, E. L., Davidson, A. R., and Forman-Kay, J. D. (2001) Dramatic stabilization of an SH3 domain by a single substitution: Roles of the folded and unfolded states, *J. Mol. Biol. 307*, 913−928.
25. Klein-Seetharaman, J., Oikawa, M., Grimshaw, S. B., Wirmer, J., Duchardt, E., Ueda, T., Imoto, T., Smith, L. J., Dobson, C. M., and Schwalbe, H. (2002) Long-range interactions within a nonnative protein, *Science 295*, 1719−1722.
26. Barua, B., and Andersen, N. H. (2001) Determinants of miniprotein stability: Can anything replace a buried H-bonded Trp sidechain? *Lett. Pept. Sci. 8*, 221−226.
27. Bothnerby, A. A., Stephens, R. L., Lee, J. M., Warren, C. D., and Jeanloz, R. W. (1984) Structure Determination of a Tetrasaccharide: Transient Nuclear Overhauser Effects in the Rotating Frame, *J. Am. Chem. Soc. 106*, 811−813.
28. Hull, W. E., and Sykes, B. D. (1976) Fluorine-19 Nuclear Magnetic-Resonance Study of Fluorotyrosine Alkaline-Phosphatase: Influence of Zinc on Protein Structure and a Conformational Change Induced by Phosphate Binding, *Biochemistry 15*, 1535−1546.
29. Frieden, C. (2003) The kinetics of side chain stabilization during protein folding, *Biochemistry 42*, 12439−12446.
30. Shu, Q., and Frieden, C. (2004) Urea-dependent unfolding of murine adenosine deaminase: Sequential destabilization as measured by F-19 NMR, *Biochemistry 43*, 1432−1439.

31. Shu, Q., and Frieden, C. (2005) Relation of enzyme activity to local/global stability of murine adenosine deaminase: F-19 NMR studies, *J. Mol. Biol. 345*, 599−610.
32. Danielson, M. A., Biemann, H. P., Koshland, D. E., and Falke, J. J. (1994) Attractant-Induced and Disulfide-Induced Conformational-Changes in the Ligand-Binding Domain of the Chemotaxis Aspartate Receptor: A F-19 Nmr-Study, *Biochemistry 33*, 6100−6109.
33. Truong, H. T. N., Pratt, E. A., and Ho, C. (1991) Interaction of the Membrane-Bound D-Lactate Dehydrogenase of *Escherichia coli* with Phospholipid Vesicles and Reconstitution of Activity Using a Spin-Labeled Fatty Acid as an Electron Acceptor: A Magnetic Resonance and Biochemical Study, *Biochemistry 30*, 3893−3898.
34. Danielson, M. A., and Falke, J. J. (1996) Use of F-19 NMR to probe protein structure and conformational changes, *Annu. Rev. Biophys. Biomol. Struct. 25*, 163−195.
35. Rule, G. S., Pratt, E. A., Simplaceanu, V., and Ho, C. (1987) Nuclear Magnetic Resonance and Molecular Genetic Studies of the Membrane-Bound D-Lactate Dehydrogenase of *Escherichia coli*, *Biochemistry 26*, 549−556.
36. Gerig, J. T. (1994) Fluorine NMR of Proteins, *Prog. Nucl. Magn. Reson. Spectrosc. 26*, 293−370.
37. Prosser, R. S., Luchette, P. A., and Westerman, P. W. (2000) Using O_2 to probe membrane immersion depth by F-19 NMR, *Proc. Natl. Acad. Sci. U.S.A. 97*, 9967−9971.
38. Prosser, R. S., Luchette, P. A., Westerman, P. W., Rozek, A., and Hancock, R. E. W. (2001) Determination of membrane immersion depth with O_2: A high-pressure F-19 NMR study, *Biophys. J. 80*, 1406−1416.
39. Luchette, P. A., Prosser, R. S., and Sanders, C. R. (2002) Oxygen as a paramagnetic probe of membrane protein structure by cysteine mutagenesis and F-19 NMR spectroscopy, *J. Am. Chem. Soc. 124*, 1778−1781.
40. Esposito, G., Lesk, A. M., Molinari, H., Motta, A., Niccolai, N., and Pastore, A. (1992) Probing Protein Structure by Solvent Perturbation of Nuclear Magnetic Resonance Spectra: Nuclear Magnetic Resonance Spectral Editing and Topological Mapping in Proteins by Paramagnetic Relaxation Filtering, *J. Mol. Biol. 224*, 659−670.
41. Piotto, M., Saudek, V., and Sklenar, V. (1992) Gradient-Tailored Excitation for Single-Quantum NMR Spectroscopy of Aqueous Solutions, *J. Biomol. NMR 2*, 661−665.
42. Bertini, I., Dalvit, C., Huber, J. G., Luchinat, C., and Piccioli, M. (1997) ePHOGSY experiments on a paramagnetic protein: Location of the catalytic water molecule in the heme crevice of the oxidized form of horse heart cytochrome c, *FEBS Lett. 415*, 45−48.
43. Dalvit, C. (1998) Efficient multiple-solvent suppression for the study of the interactions of organic solvents with biomolecules, *J. Biomol. NMR 11*, 437−444.
44. Tollinger, M., Skrynnikov, N. R., Mulder, F. A. A., Forman-Kay, J. D., and Kay, L. E. (2001) Slow dynamics in folded and unfolded states of an SH3 domain, *J. Am. Chem. Soc. 123*, 11341−11352.
45. Minks, C., Huber, R., Moroder, L., and Budisa, N. (1999) Atomic mutations at the single tryptophan residue of human recombinant annexin V: Effects on structure, stability, and activity, *Biochemistry 38*, 10649−10659.
46. Amovilli, C., and Floris, F. M. (2003) Solubility of water in liquid hydrocarbons: A bridge between the polarizable continuum model and the mobile order theory, *Phys. Chem. Chem. Phys. 5*, 363−368.
47. Shea, J. E., Onuchic, J. N., and Brooks, C. L. (2002) Probing the folding free energy landscape of the src-SH3 protein domain, *Proc. Natl. Acad. Sci. U.S.A. 99*, 16064−16068.
48. Guo, W. H., Lampoudi, S., and Shea, J. E. (2003) Posttransition state desolvation of the hydrophobic core of the src-SH3 protein domain, *Biophys. J. 85*, 61−69.
49. Cheng, Y. K., and Rossky, P. J. (1998) Surface topography dependence of biomolecular hydrophobic hydration, *Nature 392*, 696−699.
50. Svergun, D. I., Richard, S., Koch, M. H. J., Sayers, Z., Kuprin, S., and Zaccai, G. (1998) Protein hydration in solution: Experimental observation by X-ray and neutron scattering, *Proc. Natl. Acad. Sci. U.S.A. 95*, 2267−2272.
51. Altenbach, C., Greenhalgh, D. A., Khorana, H. G., and Hubbell, W. L. (1994) A Collision Gradient Method to Determine the Immersion Depth of Nitroxides in Lipid Bilayers: Application to Spin-Labeled Mutants of Bacteriorhodopsin, *Proc. Natl. Acad. Sci. U.S.A. 91*, 1667−1671.
52. Al-Abdul-Wahid, M. S., Yu, C.-H., Batruch, I., Evanics, F., Pomes, R., and Prosser, R. S. (2006) A Combined NMR and Molecular Dynamics Study of the Transmembrane Solubility and Diffusion Rate Profile of Dioxygen in Lipid Bilayers, *Biochemistry 45*, 10719−10728.
53. Dalvit, C. (1995) New One-Dimensional Selective NMR Experiments in Aqueous Solutions Recorded with Pulsed-Field Gradients, *J. Magn. Reson., Ser. A 113*, 120−123.
54. Evanics, F., Hwang, P. M., Cheng, Y., Kay, L. E., and Prosser, R. S. (2006) Topology of an outer-membrane enzyme: Measuring oxygen and water contacts in solution NMR studies of PagP, *J. Am. Chem. Soc. 128*, 8256−8264.
55. Schroder, C., Rudas, T., Boresch, S., and Steinhauser, O. (2006) Simulation studies of the protein-water interface. I. Properties at the molecular resolution, *J. Chem. Phys. 124*.
56. Rudas, T., Schroder, C., Boresch, S., and Steinhauser, O. (2006) Simulation studies of the protein-water interface. II. Properties at the mesoscopic resolution, *J. Chem. Phys. 124*.
57. Dalvit, C., and Hommel, U. (1995) New Pulsed-Field Gradient NMR Experiments for the Detection of Bound Water in Proteins, *J. Biomol. NMR 5*, 306−310.

BI061389R